Electron-Molecule Collisions:Quantitative Approaches and the Legacy of Aaron Temkin

B. I. Schneider*
Physics Division, National Science Foundation, Arlington, Virginia 22230 and Electron and Optical Physics Division, National Institute of Standards and Technology, Gaithersburg, MD 20899

I. INTRODUCTION

This article, on electron-molecule collisions, is dedicated to the legacy of my good friend and sometime collaborator, Aaron Temkin on his retirement from the NASA-Goddard Space Flight Center after many years of work at the highest intellectual level in the theoretical treatment of electron-atom and electron-molecule scattering. Aaron's contributions to the manner in which we think about electron-molecule collisions is clear to all of us who have worked in this field. I doubt that the great progress that has occurred in the computational treatment of such complex collision problems could have happened without these contributions. For a brief historical account, see the discussion of Temkin's contribution to electron-molecule scattering in the first article of this volume by Dr. A. K. Bhatia.

In this article, I will concentrate on the application of the so called, non-adiabatic R-matrix theory, to vibrational excitation and dissociative attachment, although I will also present some results applying the Linear Algebraic and Kohn-Variational methods to vibrational excitation. As a starting point for almost all computationally effective approaches to electron-molecule collisions, is the fixed nuclei approximation. That is, one recognizes, just as one does with molecular bound states, that there is a separation of electronic(fast) and nuclear(slow) degrees of freedom. This separation makes it possible to "freeze" the nuclei in space, calculate the collision parameters for the frozen molecule and then, somehow to add back the vibrations and rotations. The manner in which this is done, depends on the details of the collision problem. It is the work of Aaron and a number of other researchers that has provided the guidance necessary to resolve these issues.

II. THE FIXED NUCLEI PROBLEM

A. Geometric Considerations

Let us first consider the relationship between a coordinate system whose origin is centered at the center of mass of a molecule and the laboratory frame of reference. The laboratory frame of reference is illustrated in Figure 1, where the z' axis is defined to lie along the incident electron beam direction and the scattered beam is in the direction (θ', ϕ') relative to this direction. The molecular frame of reference, which is rigidly attached to the molecule, is illustrated

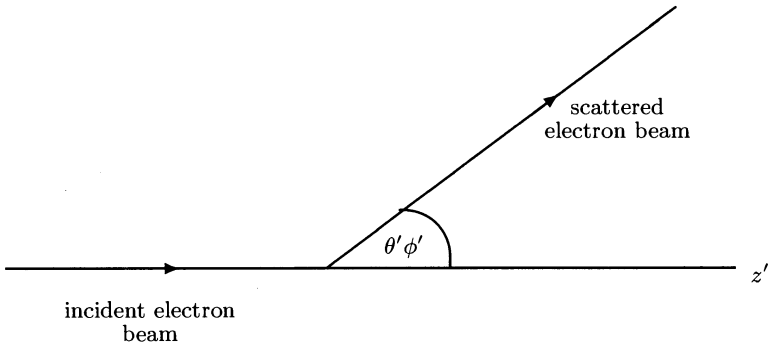

*Electronic address: bschneid@nsf.gov

FIG. 1: Laboratory frame for electron molecule scattering.

in Figure 2 for the case of a diatomic molecule. The center of gravity, G, is chosen as the origin of coordinates, with the z-axis lying along the internuclear axis, R, and the two nuclei labelled as A and B, $R = R_A + R_B$. For a general

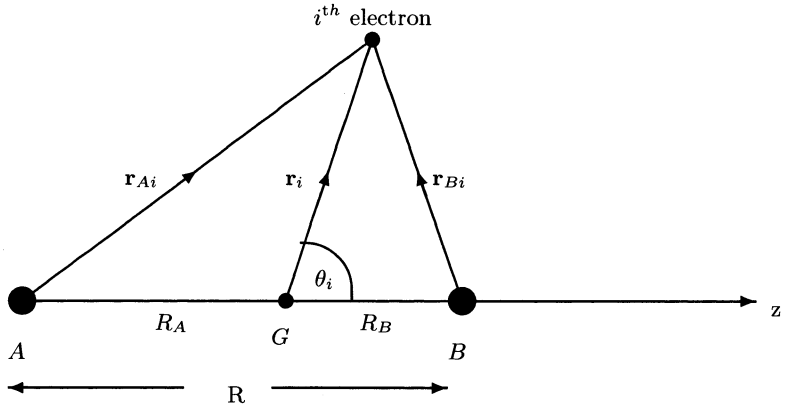

FIG. 2: Molecular frame for electron diatomic molecule collisions.

polyatomic molecule, one would choose the principle axis of inertia to replace the z-axis of the diatomic molecule. The molecular frame is oriented in a direction defined by the Euler angles α, β, γ, discussed, for example, in [33], which takes the laboratory frame of reference into the molecular frame of reference. Almost all electron-molecule scattering calculations are carried out in the molecular reference frame, where it is more natural to treat short-range effects such as exchange and correlation in non-vibrating, non-rotating molecules. Physical quantities, such as scattering amplitudes and cross sections, are extracted from the asymptotic form of the scattering wavefunction, which is typically written in a spherical coordinate system attached to the molecular frame. Consequently, it is necessary to transform the asymtotic form of the scattering wavefunction from the molecular to the laboratory reference frame. All that is required to perform this transormation is,

$$Y_{\ell m}(\theta', \phi') = \sum_{m'} D^{\ell *}_{mm'}(\alpha, \beta, \gamma) Y_{\ell m'}(\theta, \phi), \tag{1}$$

which relates spherical harmonics in the two frames of reference, where $D^{\ell}_{mm'}(\alpha, \beta, \gamma)$ are Wigner rotation matrices, defined in [33] and α, β and γ are Euler angles which transform the laboratory frame of reference into the molecular frame of reference.

B. Dynamics: Fixed Nuclei R-Matrix Treatment

The collision process for an electron scattering from an N electron target molecule, in the fixed nuclei approximation (nuclear kinetic energy= 0), is described by the time-independent Schrödinger equation,

$$H_{N+1}\Psi^{\Gamma} = E(R)\Psi^{\Gamma}, \tag{2}$$

where H_{N+1} is the non-relativistic Hamiltonian defined in atomic units in the molecular frame where Γ designates a given irreducible representation of the molecule. In light, linear molecules, Γ is the projection of the total angular momentum along the internuclear axis. For non-linear molecules, Γ, labels the irreducible representations of the molecular point group. In most of what follows, the presentation will be for linear molecules. This simplifies the algebra but the other cases may also be treated if one admits a more cumbersome notation.

$$H_{N+1} = \sum_{i=1}^{N+1} \left(-\frac{1}{2}\nabla_i^2 - \frac{Z_A}{r_{Ai}} - \frac{Z_B}{r_{Bi}} \right) + \sum_{i>j=1}^{N+1} \frac{1}{r_{ij}} + \frac{Z_A Z_B}{R}. \tag{3}$$

The solutions of this equation depend parametrically on R. There have been a number of successful approaches developed over the past few decades to calculating accurate, ab-initio, wavefunctions to eq(2). Early researchers used

single-center expansions ([1, 2]) and solved the resultant set of coupled, integro-differential equations using Numerov or related numerical integration procedures. Others turned to integral equation formulations. However, the most robust methods were based on multi-center expansions and variational methods to reduce the problem to one of linear algebra. Techniques such as the R-matrix ([7–9]) and Kohn Variational method ([3, 4]) expand the wavefunction in a computationally convenient basis set, substitute the expansion into the Schrödinger equation, and use projection techniques to obtain algebraic equations for the expansion coefficients. In the R-matrix method, which we describe in detail below, the major computational effort is spent solving an eigenvalue problem. In the Kohn Variational method, one is faced with solving a set of real or complex linear algebraic equations. The solution of eq(2) is typically expanded in a set of basis functions designed to explicitly represent channels that are energetically accessible(open channels/P-space) and those that are not (closed channels/Q-space). The P-space components asymptotically contain the scattering information while the Q-space components are needed to describe certain exchange effects, polarization and electron correlation. Often the physical closed states are replaced by pseudostates, which are better adapted to describing these effects using a much smaller set of basis functions. The common characteristic of Q-space basis functions is that they exponentially decay far from the interaction region. It has also become common to include in the expansion pseudostates designed to represent high lying, open channels in the breakup region of the target molecule. These non-physical states are needed to represent, in some fashion, the loss of flux into the continuum. We typically define the P-space basis functions as,

$$\psi^{\Gamma}_{c,i} = \mathcal{A}[\Phi^{\Gamma}_{c}(\mathbf{X}_N;\hat{\mathbf{r}}_{N+1}\sigma_{N+1})u^{0}_{c,i}(r_{N+1})] \tag{4a}$$

$$\Phi^{\Gamma}_{c}(\mathbf{X}_N;\hat{\mathbf{r}}_{N+1}\sigma_{N+1}) = \Phi^{SM_S}_{c}(\mathbf{X}_N;\sigma_{N+1})Y_{\ell_c m_{\ell_c}}(\theta_{N+1},\phi_{N+1}) \tag{4b}$$

$$\Phi^{SM_S}_{c}(\mathbf{X}_N;\sigma_{N+1}) = \sum_{M_{S_c}m_c}\Phi_c(\mathbf{X}_N)\chi_{\frac{1}{2}m_c}(\sigma_{N+1})(S_cM_{S_c}\tfrac{1}{2}m_c|SM_S), \tag{4c}$$

and the Q-space wavefunctions as, $\chi^{\Gamma}_{q}(\mathbf{X}_{N+1})$. Note, that the P-space basis states are constructed as an antisymmetrized product of a set of n physical target states and m one-electron function representing the scattering electron. The channel functions are here taken to be eigenfunctions of total spin S of the $(N+1)$ electron system and its projection, M_S, on the z-axis. The number, M, of Q-space wavefunctions is, in principle, arbitrary, but in practice is restricted to keep the size of the overall expansion manageable. At a minimum, the Q-space states must include enough functions to keep the P and Q space parts of the overall expansion orthogonal. In the R-matrix approach, the one-electron functions may be regular solutions to some model eigenvalue problem, designed to improve convergence of the expansion, but simpler forms may also be employed. The P-space wavefunctions are orthonormal and that requires that certain orthogonality conditions be imposed on the $u^{0}_{c,i}$ one-electron basis. In the Kohn Variational method, the one-electron functions are chosen as unknown linear combinations of asymptotically regular and irregular solutions of either the non-interacting problem or some model problem. Again, there are certain orthogonality conditions that need to be imposed to make the expansion numerically tractable. The linear combination is determined using the Kohn Variational principle. In the R-matrix approach, first developed in [7, 8], the major computational step is the solution of the composite $(N+1)$ electron eigenvalue problem,

$$\left[H_{N+1}+L_{N+1}-E_k(R)\right]\Psi^{\Gamma}_{k}=0 \tag{5a}$$

$$\Psi^{\Gamma}_{k}=\sum_{c=1}^{n}\sum_{i=1}^{m}\psi^{\Gamma}_{c,i}a_{c,i,k}+\sum_{q=1}^{M}\chi^{\Gamma}_{q}b_q \tag{5b}$$

where we have dropped the coordinate labels for notational simplicity. Note, that all the electron coordinates are restricted to lie inside a sphere of radius $r\leq a_0$. Inside the sphere, the composite system is subject to the full dynamical range of effects such as exchange, and short range correlation. Outside the sphere, pure electrostatic effects dominate the interaction of the target and the scattered electron and antisymmetry of target and scattered electron may be ignored. The Bloch operator, L, in eq(5) is defined as,

$$L_{N+1}=\sum_{i=1}^{N+1}\frac{1}{2}\delta(r_i-a)\left(\frac{\partial}{\partial r_i}-b\right), \tag{6}$$

where b is an arbitrary, real constant. One can demonstrate that $H_{N+1}+L_{N+1}$ is Hermitian in a basis of square integrable functions satisfying arbitrary boundary conditions at $r=a_0$. The major computational advantage of the R-matrix approach is its similarity to standard bound state eigenvalue problems. Inside $r=a_0$, the wavefunction may be expanded in a convenient set of basis functions and the problem reduced to the diagonalization of a matrix. The one and two electron integrals are defined inside $r=a_0$ and while most of these matrix elements have a negligible contribution from regions outside $r=a_0$, others must be treated more carefully. For those matrix elements involving

orbitals that have an appreciable contribution from regions $r \geq a_0$, the procedure is to compute the integrals over all of space and subtract the part for $r \geq a_0$. Typically, the subtraction may be done using multipolar expansions and is inexpensive as long as the number of integrals is not too large. In the modern R-matrix codes, all of the orbitals are expanded in a set of multicenter Gaussian type orbitals. The R-matrix orbitals, which must have significant amplitude at $r = a_0$, contain diffuse Gaussians placed at the center of gravity of the molecule for all of the asymptotically important partial waves. For the details see [27, 28]. We now employ the expansion of eq(5b) to solve the scattering problem at energy $E(R)$ in the internal region.

$$\left[H_{N+1} + L_{N+1} - E(R)\right]\Psi^{\Gamma} = L_{N+1}\Psi^{\Gamma} \tag{7a}$$

$$\Psi^{\Gamma} = \sum_k \frac{\Psi_k^{\Gamma}}{[E_k(R) - E(R)]} \langle \Psi_k^{\Gamma} \mid L_{N+1} \mid \Psi^{\Gamma} \rangle \tag{7b}$$

In order to extract the scattering information from this equation, we project Ψ^{Γ} onto the channel functions, $\Phi_c^{\Gamma}(\mathbf{X}_N; \hat{\mathbf{r}}_{N+1}\sigma_{N+1})$ and then set $r_{N+1} = a_0$. This produces the following set of coupled, *algebraic equations.*

$$u_c(a_0) = \sum_{d=1}^{n} \mathcal{R}_{c,d}\left[\frac{\partial u_d(r)}{\partial r} - b u_d(r)\right]|_{r=a_0} \tag{8}$$

In the above equation the radial scattering functions are defined as,

$$u_c(r_{N+1}) = \left(\Phi_c^{\Gamma}(\mathbf{X}_N; \hat{\mathbf{r}}_{N+1}\sigma_{N+1}) \mid \Psi^{\Gamma}(\mathbf{r}_1, \mathbf{r}_2, ...\mathbf{r}_{N+1})\right) \tag{9}$$

and the R-matrix matrix elements as,

$$\begin{aligned} \mathcal{R}_{c,d} &= \frac{1}{2}\sum_k \frac{u_{c,k}(a_0)u_{d,k}(a_0)}{[E_k(R) - E(R)]} \\ u_{c,k}(a_0) &= \sum_i a_{c,i,k} u_{c,i}^0(a_0) \end{aligned} \tag{10}$$

The only remaining task, is to solve these equations and extract the scattering information. To accomplish that requires us to consider the form of the scattering equations in the long-range region. Since the scattered and target electrons are now separated in space, the relevant equations are,

$$\left(\frac{d^2}{dr^2} - \frac{\ell_c(\ell_c+1)}{r^2} + \frac{2(Z_A + Z_B - N)}{r} + k_c^2\right) u_c(r) = 2\sum_{d=1}^{n} V_{c,d}(r) u_d(r) \tag{11}$$

$$k_c^2 = 2(E - E_c)$$

The simplest approach to dealing with these equations is to use the R-matrix method in the external region(s). Consider the region between the two annuli, $r = a_0$ and $r = b_0$. Lets us assume we have already calculated the R-matrix, $\mathbf{R}^I$, from $r = 0$ to $r = a_0$. Using the continuity of the functions and their first derivatives on the interval (a_0, b_0), joining the regions, it is possible to derive an equation for the R-matrix, $\mathbf{R}^{I+1}$, from $r = 0$ to $r = b_0$. This approach, known as the R-matrix propagation method, has a long history in heavy particle collisions [29, 32] and was adapted to electron-atom and electron-molecule scattering by a number of authors [30, 31]. I only quote the fundamental equation,

$$\mathbf{R}^{I+1} = \mathbf{r}_{b_0,b_0}^{I+1} - \mathbf{r}_{b_0,a_0}^{I+1}\left[\mathbf{R}^I + \mathbf{r}_{a_0,a_0}^{I+1}\right]^{-1}\mathbf{r}_{a_0,b_0}^{I+1} \tag{12}$$

where the $\mathbf{r}_{q,q'}^{I+1}$ are the sub-region R-matrices relating the adjacent boundaries, $r = a_0$ and $r = b_0$. Once we have propagated the R-matrix into the far asymptotic region, it can be matched to known analytic forms. At these distances the equations have two linearly independent solutions which may be obtained by a variety of methods; inward numerical integration, inverse power series expansions, analytic techniques or combinations of all of these, depending on the distance. Which linearly independent solutions are used depends on what boundary conditions are imposed on the solution in the far asymptotic region. The easiest ones to deal with impose the conditions that,

$$u_c(r) \underset{r\to\infty}{\sim} k_c^{-\frac{1}{2}}(\delta_{c,d}\sin(\theta_c r) + \cos(\theta_c r)K_{c,d}^{\Gamma}) \tag{13}$$

$$\theta_c = k_c r - \frac{1}{2}\ell_c\pi - \eta_c \ln 2k_c r + \sigma_{\ell_c}$$

Substituting this into eq(8), rearranging terms, leads to an equation for unknown $K_{c,d}$. Other asymptotic forms may easily obtained using the standard relations,

$$\mathbf{S}^{\Gamma} = \left[\mathbf{I} - i\mathbf{K}^{\Gamma}\right]^{-1}\left[\mathbf{I} + i\mathbf{K}^{\Gamma}\right] \tag{14a}$$

$$\mathbf{T}^{\Gamma} = \mathbf{S}^{\Gamma} - \mathbf{I} \tag{14b}$$

In order to obtain the scattering amplitude, it is necessary to express the asymptotic solution as a linear combination of an incident plane wave in channel c plus an outgoing spherical wave in all the open channels, in the laboratory coordinate system.

$$\Psi_c = \Psi_c^{\rm inc} + \Psi_c^{\rm scatt} \tag{15a}$$

$$\Psi_c^{\rm inc} \underset{r'_{N+1}\to\infty}{\sim} \Phi_c(\mathbf{X}_N)\chi_{\frac{1}{2}m_c}(\sigma_{N+1})\exp(ik_c z'_{N+1}) = \tag{15b}$$

$$\frac{i\pi^{1/2}}{k_c r'_{N+1}}\sum_{S\ell_c} i^{\ell_c}(2\ell_c+1)^{\frac{1}{2}}\Phi_c^{SM_S}(\mathbf{X}_N;\sigma_{N+1})(S_c M_{S_c}\tfrac{1}{2}m_c|SM_S)\times(\exp(-i\theta'_c)-\exp(i\theta'_c))Y_{\ell_c 0}(\theta'_{N+1},0),$$

$$\Psi_c^{\rm scatt} \underset{r'_{N+1}\to\infty}{\sim} \sum_d \Phi_d(\mathbf{X}_N)\chi_{\frac{1}{2}m_d}(\sigma_{N+1})f_{dc}(\theta'_{N+1},\phi'_{N+1})\frac{\exp(ik_d r'_{N+1})}{r'_{N+1}}, \tag{15c}$$

The remaining task is to determine the linear combination of molecular frame solutions, needed to reproduce the incoming laboratory frame plane wave of eq(15b). To accomplish this we write,

$$\Psi_c = \sum_{\Gamma} A_c^{\Gamma}\Psi_c^{\Gamma} \tag{16a}$$

$$\Psi_c^{\Gamma} = \sum_d \left[\Phi_d^{\Gamma}(\mathbf{X}_N;\hat{\mathbf{r}}_{N+1}\sigma_{N+1})\Phi_d^{SM_S}(\mathbf{X}_N;\sigma_{N+1})Y_{\ell_d m_{\ell_d}}(\theta_{N+1},\phi_{N+1})u_{dc}(r_{N+1})\right] \tag{16b}$$

$$u_{dc} \underset{r\to\infty}{\sim} \exp(-i\theta_d)\delta_{c,d} - S_{dc}\exp(-i\theta_d) \tag{16c}$$

Inserting eq(16c) into eq(16b) and then substituting the result into eq(16a), results in an asymptotic expression for Ψ_c expressed in the molecular reference frame. By choosing,

$$A_c^{\Gamma} = i\pi^{1/2}k_c^{-1/2}i^{\ell_c}(2\ell_c+1)^{\frac{1}{2}}(S_c i M_{S_c}\tfrac{1}{2}m_c|SM_S)D^{\ell_c *}_{0m_{\ell_c}}(\alpha,\beta,\gamma). \tag{17}$$

and using eq(1) it is possible to demonstrate that we indeed produce the required incident wave in the laboratory reference frame. To my knowledge, this was first demonstrated in a slightly simpler form in the paper of Temkin and Vasavada[5]. The scattering amplitude may immediately be extracted as,

$$f_{dc}(\theta',\phi') = -i\left(\frac{\pi}{k_c k_d}\right)^{1/2}\sum_{\Lambda S\pi}\sum_{\ell_c m_{\ell_c}\ell_d m_{\ell_d} m_{\ell_{d'}}} i^{\ell_c-\ell_d}(2\ell_c+1)^{\frac{1}{2}}(S_c M_{S_c}\tfrac{1}{2}m_c|SM_S)$$
$$\times(S_d M_{S_d}\tfrac{1}{2}m_d|SM_S)T^{\Gamma}_{dc}D^{\ell_c *}_{0m_{\ell_c}}(\alpha,\beta,\gamma)D^{\ell_d}_{m_{\ell_{d'}}m_{\ell_d}}(\alpha,\beta,\gamma)Y_{\ell_d m_{\ell_{d'}}}(\theta',\phi'), \tag{18}$$

In the fixed nuclei approximation, the scattering amplitude depends parametrically on the nuclear coordinates. In keeping with the philosophy of the Born-Oppenheimer approximation, transitions between electronic, vibrational and rotational states of the molecule may be obtained from these amplitudes by simply multiplying by the appropriate ro-vibrational wavefunctions of the target and integrating over the nuclear degrees of freedom. This approach, the so-called adiabatic-nuclei approximation, was first discussed in [34–36], and is valid provided the collision time is short compared with the times for vibration and/or rotation of the neutral molecule. Hence it can be applied in non-resonant regions or at electron collision energies which are not close to threshold. In the case of diatomic molecules in a $^1\Sigma$ state the scattering amplitude for a transition between electronic, vibrational and rotational states defined by the quantum numbers $c\nu_c j_c m_{j_c}$ and $d\nu_d j_d m_{j_d}$ is given by

$$f_{d\nu_d j_d m_{j_d},c\nu_c j_c m_{j_c}}(\mathbf{k}\cdot\hat{\mathbf{r}}) = \langle\chi_{\nu_d}(R)Y_{j_d,m_{j_d}}(\hat{\mathbf{R}})|f_{dc}(\theta',\phi')|\chi_{\nu_c}(R)Y_{j_c m_{j_c}}(\hat{\mathbf{R}})\rangle, \tag{19}$$

where $f_{dc}(\theta',\phi')$ is defined in 18. In this approximation both the rotational and vibrational degress of freedom are assumed to follow the adiabatic-nuclei prescription. In many cases, the prescription is not valid for the vibrational degrees of freedom but is an excellent approximation for the slower rotations. A hybrid theory was developed in [6, 21] to account for such a situation, which occurs frequently in the vibrational excitation of molecules in the presence of electronic resonances. In this approach the electronic and vibrational degrees of freedom are *explicitly* treated using a coupled states expansion. The rotational degrees of freedom are treated as in eq. (19). An alternative approach, the non-adiabatic R-matrix method, which is also applicable to dissociative attachment, is described in the next section.

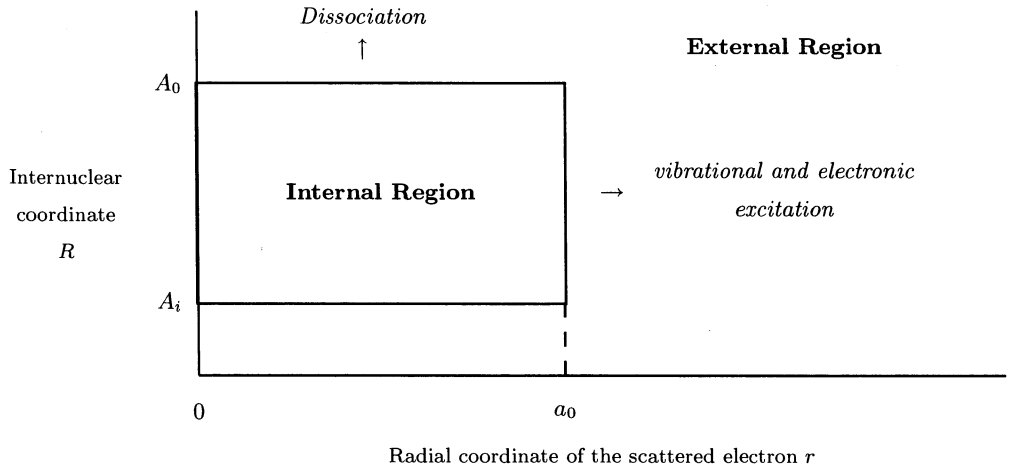

FIG. 3: Partitioning of configuration space in non-adiabatic R-matrix theory.

III. NON-ADIABATIC R-MATRIX THEORY

The adiabatic-nuclei approximation breaks down in the neighbourhood of narrow resonances or close to thresholds. This occurs because the colliding electron spends an appreciable time in the neighbourhood of the molecule allowing it to transfer energy to the nuclear motion with high probability. An interesting debate arose as to whether it was necessary to explicitly couple electronic and nuclear motion, as in a vibrational close coupling method, under these circumstances or whether a simpler conceptual and computational approach would suffice. There were formal theoretical arguments([14–17, 20]) as well as semi-empirical methods ([18]) based on the theoretical arguments that suggested this might indeed be the case, but no fully ab-initio, computational approach existed before 1979-1980. In looking back on these early papers I am quite impressed at the insight and intuition of the Manchester group. Basically, they had the physics under control. It was left to others to develop more quantitative approaches ([37, 38]) and show how first principles calculations verify these early theoretical developments.

We now consider the time-independent Schrödinger equation for a diatomic molecule,

$$(H_{N+1} + T_R)\Psi\mathbf{X}_{N+1}, R) = E\Psi(\mathbf{X}_{N+1}, R), \tag{20}$$

where we explicitly include the nuclear kinetic energy operator,

$$T_R = -\frac{1}{2\mu}\frac{d^2}{dR^2}, \tag{21}$$

and μ is the reduced mass of the two nuclei. We will assume that the molecule does not rotate appreciably during the collision. In Figure 3 we illustrate the partitioning of configuration space adopted in non-adiabatic R-matrix theory. The internal region is taken to be a rectangle defined by $0 \leq r \leq a_0$ and $A_i \leq R \leq A_0$ where a_0 is defined in the same way as in the fixed-nuclei theory given in Section II, A_i is chosen to exclude the nuclear Coulomb repulsion singularity at $R = 0$, where the wave function describing the nuclear motion is negligible, and A_0 is chosen so that the target vibrational states of interest in the calculation have negligible amplitude for $R > A_0$. For $r > a_0$ the molecule separates into an electron plus residual molecule which may be vibrationally and/or electronically excited. For $R > A_0$ the molecule separates into an atom plus an atomic negative ion (dissociative attachment) or into two free atoms plus the electron (three body breakup). In the internal region, Schrödinger equation, takes the form,

$$(H_{N+1} + T_R + L_{N+1} + L_R - E)\Psi^\Gamma(\mathbf{X}_{N+1}, R) = E\Psi^\Gamma(\mathbf{X}_{N+1}, R) \tag{22}$$

where the Bloch operators L_{N+1} and L_R are introduced so that $H_{N+1} + T_R + L_{N+1} + L_R$ is hermitian in the basis of quadratically integrable functions defined over the internal region in Figure 3 and satisfying arbitrary boundary conditions on the boundary of this region. We have already defined L_{N+1} by eq. (6) such that $H_{N+1} + L_{N+1}$ is hermitian for fixed internuclear separation R. The Bloch operator L_R, which is defined by

$$L_R = \frac{1}{2\mu}\left[\delta(R - A_0)\left(\frac{d}{dR} - B_0\right) - \delta(R - A_i)\left(\frac{d}{dR} - B_i\right)\right], \tag{23}$$

where B_0 and B_i are arbitrary constants, is such that $T_R + L_R$ is hermitian over the range $A_i \leq R \leq A_0$. It follows that $H_{N+1} + T_R + L_{N+1} + L_R$ is hermitian as required. We now expand the total wavefunction as,

$$\Psi^\Gamma(\mathbf{X}_{N+1}; R) = \sum_k \Psi_k^\Gamma(\mathbf{X}_{N+1}; R)\Theta_k^\Gamma(R) \tag{24}$$

The Ψ_k^Γ in this equation are the fixed-nuclei R-matrix electronic basis functions defined by eq. (5b) which are solved for a mesh of fixed internuclear values of R spanning the range $A_i \leq R \leq A_0$, and the $\Theta_k^\Gamma(R)$ are functions representing the nuclear motion. Substituting eq.(24) into eq.(22), mutiplying from the left with Ψ_k^Γ, and integrating over all the electronic coordinates, produces the following equation for Θ_k^Γ, *if we ignore the derivative of the R-matrix electronic wavefunction with respect to the internuclear coordinates.*

$$\begin{aligned}
\big[T_R + L_R + E_k(R) - E\big]\Theta_k^\Gamma(R) &= \big(\Psi_k^\Gamma \mid L_{N+1} + L_R \mid \Psi^\Gamma\big) \\
&= \frac{1}{2}\sum_{c\nu_c} u_{c,k}(a_0, R)\chi_{\nu_c}(R)\big[\frac{\partial}{dr} - b\big]u_{c,\nu_c}(r)\mid_{r=a_0} \\
&+ \frac{1}{2\mu}\sum_{[AB]_i} u_{[AB]_i,k}(R)\delta(R - A_0)\big[\frac{\partial}{dR} - B_0\big]u_{[AB]_i}(R)
\end{aligned} \tag{25}$$

The round brackets are used to denote integrations over electronic coordinates only. The two summations are respectively over 1) the electronic/vibrational degrees of freedom of the neutral molecule and 2) the electronically bound/dissociative degress of freedom of the negative ion. Specifically excluded from the sum are the three body states involving a true unbound outgoing electron and two dissociating nuclei, although one could include pseudostates to represent their effect just as is done in electronic breakup. This is the essence of the Born-Oppenheimer approximation and it is here applied to the internal R-matrix states of the compound $(N+1)$ particle system. The physical argument is, in the internal region, even an asymptotically slow moving electron is moving much faster than the nuclei can vibrate or rotate due to the internal electromagnetic forces experienced at small r. Mathematically, we need to examine the adiabatic potential curves for any avoided crossings. If such crossings were present, it would invalidate the argument and non Born-Oppenheimer correction terms would have to be considered to obtain quantitative agreement. The formal solution for Ψ^Γ may be written as,

$$\begin{aligned}
\Psi^\Gamma(\mathbf{X}_{N+1}, R) &= \sum_k \Psi_k^\Gamma(\mathbf{X}_{N+1}, R)\big[T_R + L_R + E_k(R) - E\big]^{-1}\big(\frac{1}{2}\sum_{c\nu_c} u_{c,k}(a_0, R)\chi_{\nu_c}(R)\big[\frac{\partial}{dr} - b\big]u_{c,\nu_c}(r)\mid_{r=a_0} \\
&+ \frac{1}{2\mu}\sum_{[AB]_i} u_{[AB]_i,k}(R)\delta(R - A_0)\big[\frac{\partial}{dR} - B_0\big]u_{[AB]_i}(R)\big)
\end{aligned} \tag{26}$$

The final step is to project this equation onto the asymptotic channel functions,

$$u_{c,\nu_c}(a_0) = \sum_{d\nu_d} \mathcal{R}_{c\nu_c,d\nu_d}\big[\frac{\partial}{dr} - b\big]u_{d,\nu_d}(r)\mid_{r=a_0} + \sum_{[AB]_i} \mathcal{R}_{c\nu_c,i}\big[\frac{\partial}{dR} - B_0\big]u_{[AB]_i}(R)\mid_{R=A_0} \tag{27a}$$

$$u_{[AB]_i}(A) = \sum_{d\nu_d} \mathcal{R}_{i,d\nu_d}\big[\frac{\partial}{dr} - b\big]u_{d,\nu_d}(r)\mid_{r=a_0} + \sum_{[AB]_j} \mathcal{R}_{i,j}\big[\frac{\partial}{dR} - B_0\big]u_{[AB]_j}(R)\mid_{R=A_0} \tag{27b}$$

$$\mathcal{R}_{c\nu_c,d\nu_d} = \frac{1}{2}\sum_k \big\langle \chi_{\nu_c}(R)u_{c,k}(a_0, R) \mid G_k(R \mid R') \mid u_{d,k}(a_0, R')\chi_{\nu_d}(R')\big\rangle \tag{27c}$$

$$\mathcal{R}_{c\nu_c,i} = \frac{1}{2\mu}\sum_k \big\langle \chi_{\nu_c}(R)u_{c,k}(a_0, R) \mid G_k(R \mid A_0)\big\rangle \mid u_{[AB]_i,k}(A_0) \tag{27d}$$

$$\mathcal{R}_{i,c\nu_c} = \frac{1}{2}\sum_k u_{[AB]_i,k}(A_0)\big\langle G_k(A_0 \mid R)\chi_{\nu_c}(R)u_{c,k}(a_0, R)\big\rangle \tag{27e}$$

$$\mathcal{R}_{i,j} = \frac{1}{2\mu}\sum_k u_{[AB]_i,k}(R_0)G_k(A_0 \mid A_0)u_{[AB]_j,k}(A_0) \tag{27f}$$

$$G_k(R \mid R') = \big\langle R \mid \big[T_R + L_R + E_k(R) - E\big]^{-1} \mid R'\big\rangle \tag{27g}$$

The R matrices are defined here as quadratures over the nuclear Green's operator associated with each electronic R-matrix state. In practice, they may be computed as solutions to an inhomogeneous partial differential equation

plus a qudrature or by using the spectral expansion of the Green's operator. The most widely used approach is to project the nuclear Hamiltonian on to a finite basis set of Gaussians or polynomials, diagonalize the resultant matrix and use the approximate eigenvalues and eigenvectors to spectrally resolve the Green's operator. Using a spectral expansion of the Green's operator,

$$G_k(R \mid R') = \sum_q \mid \theta_{k,q}(R)\rangle\big[\epsilon_{k,q} - E\big]^{-1}\langle\theta_{k,q}(R') \mid \tag{28}$$

the R-matrices may be rewitten as,

$$\mathcal{R}_{c\nu_c,d\nu_d} = \frac{1}{2}\sum_{k,q}\big\langle\chi_{\nu_c}(R) \mid u_{c,k}(a_0,R) \mid \theta_{k,q}(R)\big\rangle\big[\epsilon_{k,q} - E\big]^{-1}\big\langle\theta_{k,q}(R') \mid u_{d,k}(a_0,R') \mid \chi_{\nu_d}(R')\big\rangle \tag{29a}$$

$$\mathcal{R}_{c\nu_c,i} = \frac{1}{2\mu}\sum_{k,q}\big\langle\chi_{\nu_c}(R) \mid u_{c,k}(a_0,R) \mid \theta_{k,q}(R)\big\rangle\big\langle\theta_{k,q}(A_0) \mid \big[\epsilon_{k,q} - E\big]^{-1} \mid u_{[AB]_i,k}(A_0) \tag{29b}$$

$$\mathcal{R}_{i,c\nu_c} = \frac{1}{2}\sum_{k} u_{[AB]_i,k}(A_0) \mid \theta_{k,q}(A_0)\big\rangle\big[\epsilon_{k,q} - E\big]^{-1}\big\langle\theta_{k,q}(R) \mid u_{c,k}(a,R) \mid \chi_{\nu_c}(R)\big\rangle \tag{29c}$$

$$\mathcal{R}_{i,j} = \frac{1}{2\mu}\sum_{k} u_{[AB]_i,k}(R_0) \mid \theta_{k,q}(A_0)\big\rangle\big[\epsilon_{k,q} - E\big]^{-1}\big\langle\theta_{k,q}(A_0) \mid u_{[AB]_j,k}(A_0) \tag{29d}$$

Note, that there is a very interesting interpretation of these equations if the variation of the electronic factors are slow and can be removed from the integration. Then, the numerators would involve Franck-Condon factors between vibrational states of the neutral and R-matrix states, while the denominators have zeros at the vibrational R-matrix eigenvalues. Thus, one might expect to see structure in the neighborhood of these zeros with an intensity dependent on the Franck-Condon factors. This is precisely what is seen in the experiments and is fundamental to the success of the Boomerang model.

The additional work required to handle the effects of nuclear motion in this non-adiabatic R-matrix method, are minimal. In particular, there is *no* explicit coupling of the electronic and vibrational degrees of freedom as happens in a vibrational close coupling technique. Perhaps more importantly, the essential readjustment of the nuclei to the environment of a long lived molecular negative ion, is built in to the R-matrix levels. There are other ab-initio approaches ([16, 17]) based on the use of Feshbach projection operator techniques, that share this important feature and also invoke the Born-Oppenheimer approximation, which have also been quite effective in treating vibrational resonances and dissociative attachment.

Once the R-matrices are computed on the surfaces on the internal region, they may be propagated outward to very large distances using a simple generalization of the methods used in the fixed nuclei case. The major difference is the need to include any additional vibrational and/or rotational coupling in the external region. Finally, links between the formal non-adiabatic R-matrix theory and the Boomerang model developed in [18], as well as quantum defect theory, may be found in the references.

IV. RESULTS

There are numerous examples of fixed nuclei electron-molecule, R-matrix theory in the literature. The number of applications of the non-adiabatic theory are much more limited but at the time the theory was developed, it was critical to demonstrate that this ab-initio approach could produce satisfactory agreement in at least one important problem, the vibrational excitation of the N_2 molecule by electrons. The problem was important for a number of reasons. First, although there were a number of vibrational excitation experiments ([10–12]) which were in essential agreement as far as the shapes and peaks in the cross sections, there were disagreements in absolute values. Experiments designed to measure the absolute value of the total cross section also existed ([13]) and those suggested that one of the vibrational excitation experiments was correct. Second, the existing theories had their own limitations. The Hybrid Theory produced qualitative agreement with the observed experimental structure but clearly was either unconverged with respect to the vibrational basis set or lacked in its treatment of the fundamental electron-molecule interaction potential. The semi-empirical Boomerang treatment does a fine job of reproducing the observed structure in the cross section but has to rely on experiment for absolute normalization. Clearly, a fully first principles treatment could and should resolve these issues. In addtion, such an approach should be able to predict as yet unmeasured cross sections such as those between excited vibrational levels. Such a calculation was undertaken while the author was on sabbatical at the Observatoire de Paris in Meudon, France in 1979-80 ([38]). The calculations were done on a CDC6600 computer at the computation center associated with the Université Paris VI. The staff there made it very easy to bring computer

codes from Los Alamos and get them running quite quickly. Almost the entire calculational effort went to computing the R-matrix eigenstates as a function of internuclear distance. The computation of the nuclear Green's operator was done using a variational/spectral approach based on Gaussian type functions. The results are shown in figure 4 to figure 9. Note in figure 4 how the R-matrix curves near the electronic resonance energy are shifted and flatter than the neutral molecule potential. This is a direct effect of the trapping of the electron into what is essentially a π_g antibonding orbital of the molecular negative ion. The results in figure 6 demonstrate the excellent agreement between the calculated and experimental results and point also to the overall normalization of the experimental results of Wong as being correct. Figure 7 comparing the current calculation with the Hybrid Theory shows that both theories have demonstrated that the resonance structure comes from the compound state state vibrational states formed in the collision complex, but the Hybrid Theory calculation has been unable to capture the details. I believe it is a consequence of expanding the scattering wavefunction in the vibrational basis of the neutral molecule. This is slowly convergent in the resonance region and would require a large number of states to reproduce the experimental features. Also shown, are the vibrational cross sections from excited state vibrational levels and the total cross section. The agreement between the R-matrix theory and experiment is gratifying and gives us confidence in the non-adiabatic R-matrix theory.

I will conclude this paper with some examples using the Linear Algebraic (LAM) and Complex Kohn Variational Method (CKVM) to calculate electron-molecule scattering cross section in diatomic and polyatomic systems. The discussion, by necessity, will be brief and the interested reader should consult the references for more details.

A fundamental problem in electron-molecule collisions is to compute reliable cross sections for electronic excitation. The transition from the ground X $^1\Sigma_g^+$ to the b $^3\Sigma_u^+$ of H_2 had been studied experimentally ([39–41] as well as computationally ([42] by a number of researchers . Early theoretical calculations agreed with one of the three experimental results but differed by a factor of two from the other two experiments. Since both the LAM, R-matrix and Schwinger Variational Method had matured enough to perform the calculation with all the relevant electron-molecule terms included, this calculation was undertaken by all three groups ([43–45]. The relevant thoretical and experimental data is shown in figure 10. The three theoretical results were in perfect agreement with one another but disagreed with the earlier theoretical calculation. The calculations also agreed with two of the experimental measurements. This work prompted the third experimental group to re-examine its measurements. It was discovered that these experimental measurements were, in fact, normalized incorrectly. When this was corrected all of the theoretical calculations and all of the experiments agreed. This was very strong evidence of the importance and need of precise calculations where experiments are difficult and uncertainties abound.

Another interesting problem involves the doubly excited $^1\Pi_u$ states of the H_2 molecule. In fig 11 ([46]), we see that there there are two series ($1\sigma_u n\pi_g^+$) and ($1\pi_u^+ n\sigma_g$) which cross as a function of internuclear distance. This must occur if one examines the behavior of the orbitals in the separated and united atom limits. Calculations on the two separate series show very different behavior of the widths of these resonances, one tending to be broad and the other narrow. The question is, if configuration interaction (CI) between the two series is taken into account, do the multiple crossings of these series produce interesting and possibly observable effects. The answer, shown by the calculations, is that CI radically changes the simple picture of two separate resonance series. The widths vary dramatically as a function of R, due to the level crossings. A photoionization experiment was proposed to probe the interesting regions of R using vibrationally excited H_2 but for technical reasons, the experiment could not be performed. It is difficult to prepare vibrationally excited homonuclear molecules experimentally. Nonetheless, this theoretical calculation again demonstrated that powerful computational methods and theory can bring a great deal of insight into electron collisions and photoionization of molecular systems.

Turning to the CKVM, we show in figure 12 the cross section for the elastic scattering of electrons from ethylene [47]. This was one of the earliest calculations performed on a polyatomic molecule and it incorporated a CI based, ab initio optical potential of a few thousand configurations to accurately treat core polarization and electron correlation. While it was expected, on general theoretical grounds, that there would be resonances involving antibonding π orbitals, an unexpected feature appeared in the cross section at very low energies; it nearly vanished. The reason for this was the existence of what is known as a Ramsauer-Townsend minimum in electron atom scattering. In a molecule the situation is not so simple as an atom, where there is spherical symmetry and only s-wave scattering at these energies. However, the higher partial waves do not contribute much to the cross section at these low energies and the situation in this molecule is quite similar to that in the rare gas atoms. Later calculations on a variety of other polyatomic species, some hydrocarbons, some not, revealed that these minima appeared for very low energy collisions in numerous systems. The calculations appear to confirm the results of numerous swarm measurements which have appeared in the literature over many years.

Finally, in figure 13 we show the vibrational excitation of the carbon-oxygen bond in formaldehyde ([48]). Again, a CI based optical potential was employed and the calculation was carried out varying the C-O bond distance in order to treat vibration. This molecule has a low lying shape resonance, very similar to that found in N_2 and other hydrocarbons. This long lived negative ion produces a vibrational pattern similar to that shown in N_2. Coupling to

other vibrational modes in the molecule was ignored in the theoretical calculation and the vibrational motion of the C-O stretch was treated using the simple, one dimensional Boomerang model. In spite of these simplifications, the results were in quite reasonable agreement with available experiment.

V. CONCLUSION

Our ability to calculate accurate cross sections for a wide array of processes involving the collision of electrons with molecules has matured over the past decade and a half. We can now even talk about electron induced chemistry, where it is possible to follow the flow of energy deposited by an incident electron as it migrates between electronic and vibrational modes in small polyatomic molecules. Even larger systems can be treated at lower but still useful levels of approximation. The major goal is to understand how dissociation and/or dissociative attachment proceeds in these systems so that it may be controlled in a variety of important applications from the etching of computer chips to waste management. The early studies discussed in this article paved the way. Aaron Temkin played a very important role in these developments. It would be remiss of me not to mention the pioneering work of other people such as Arvid Herzenberg, Phil Burke, Howard Taylor, Norman Bardsley, and Tom O'Malley who gave us both a conceptual framework to build on as well as some useful computational tools. Aaron, I hope in your "retirement" you will continue to do science with the passion that you have always brought to your work and find even greater time for the other things you enjoy such as family, travelling and music.

---

[1] P. G. Burke and A. L. Sinfailam, J. Phys. B **3** 641 (1970)
[2] P. G. Burke and N. Chandra, J . Phys. B **5** 1696 (1972)
[3] T. N. Rescigno and B. I. Schneider, Phys. Rev. A **37**, 1044 (1988)
[4] B. I. Schneider and T. N. Rescigno, Phys. Rev. A **37**, 3749 (1988)
[5] A. Temkin, and K. V. Vasavada, Phys. Rev. **160**, 109(1960)
[6] N. Chandra and A. Temkin, Phys. Rev. A **13**, 188(1976)
[7] B. I. Schneider, Chem. Phys. Lett. **31** 237(1975)
[8] B. I. Schneider, Phys. Rev. A **11**, 1957(1975)
[9] P. G. Burke, I. Mackey and I. Shimamura, J, Phys. B **10**, 2497(1977)
[10] G. J. Schulz, Phys. Rev. **135**, A988 (1964)
[11] H. Ehrhardt and K. Willman, Z. Phys. **204**, 464 (1967)
[12] S. F. Wong and L. Dube, Phys. Rev. A **17**, 570(1978)
[13] R. E. Kennerley and R. A. Bonham, Phys. Rev. A **17**, 1844 (1978)
[14] A. Herzenberg and F. Mandl, Proc. Phys. Soc. A **270**, 48(1962)
[15] J. N.Bardsley, A. Herzenberg and F. Mandl, Proc. Phys. Soc. **89**, 321(1966)
[16] T. F. O'Malley, Phys. Rev. **150**, 14(1966)
[17] T. F. O'Malley, Phys. Rev. **156**, 230(1967)
[18] D. T. Birtwistle and A. Herzenberg, J. Phys. B **4** 53(1971)
[19] A. U. Hazi, T. N. Rescigno and M. Kurilla, Phys. Rev. A. **23** 1079(1981)
[20] B.I. Schneider, Phys. Rev. A **14**, 1923(1979)
[21] N. Chandra and A. Temkin, Phys. Rev. A **14**, 507(1976)
[22] K. L. Baluja, P.G. Burke and L. A. Morgan, Comput. Phys. Commun. **27**, 299(1982)
[23] C. Bloch, Nucl. Phys. **4**, 503(1957)
[24] P. G. Burke, A. Hibbert and W. D. Robb, J . Phys. B **4**, 153(1971)
[25] K. Pfingst, B. M. Nestmann and S. D. Peyerimhoff, J. Phys. B **27**, 2283(1994)
[26] K. Pfingst, B. M. Nestmann and S. D. Peyerimhoff, *Computational Methods for Electron-Molecule Collisions* Eds. W.M. Huo and F.A. Gianturco (Plenum Press, New York), 293(1995)
[27] L. A. Morgan, J. Tennyson, C. J. Gillan and X. Chen, X., J. Phys. B **30**, 4087(1997)
[28] L. A. Morgan, J. Tennyson, and C. J. Gillan, Comput. Phys. Commun. **114**, 120(1998)
[29] J. C. Light and R. B. Walker, J. Chem. Phys. **65**, 4272(1976)
[30] B. I. Schneider and R. B. Walker, J. Chem. Phys. **70**, 2466 (1979).
[31] B. I. Schneider and H. S. Taylor, J. Chem. Phys. **77**, 379(1982).
[32] J. C. Light, R. B. Walker, E. B. Stechel and T. G. Schmalz, Comput. Phys. Commun. **17**, 89(1979)
[33] M.E. Rose,*Elementary Theory of Angular Momentum* (John Wiley & Sons, New York, London) 1957
[34] D. M. Chase, Phys. Rev. **104**, 838 (1956)
[35] S. I. Drozdov, Sov. Phys. JETP **1**, 591 (1955)
[36] S. I. Drozdov, Sov. Phys. JETP **3**, 759 (1956)
[37] B.I. Schneider, M. LeDourneuf and P. G. Burke, J. Phys. B **12**, 1365(1979)

[38] B.I. Schneider, M. LeDourneuf and Vo Ky Lan, Phys. Rev. Lett. **43**, 1926 (1979)
[39] M. L. Khakoo, S. Trajmar, R. McAdams and W. T. Shyn, Phys. Rev. A **35**, 2832 (1986)
[40] H. Nishimura, J. Phys. Soc. Jpn **55**, 3301 (1986)
[41] R. I. Hall and L. Andric, J. Phys. B **17**, 3815 (1984)
[42] S. Chung and C. C. Lin, Phys. Rev. A **17** 1874 (1978)
[43] B.I. Schneider and L.A. Collins, J. Phys. B **18**, L857 (1985)
[44] M. A. P. Lima , T. L. Gibson , K. Takatsuka and V. McKoy, J. Phys. B **18** L865 (1985)
[45] K. L. Baluja, C. J. Noble and J. Tennyson, J. Phys. B **18** L851 (1985)
[46] L. A. Collins, B.I. Schneider, C.W. McCurdy, S. Yabushita, and C.J. Noble, Phys. Rev. Lett. **57**, 980 (1986)
[47] B. I. Schneider, T. N. Rescigno, B. H. Lengsfield and C. W. McCurdy, Phys. Rev. Lett. **66**, 2728 (1991)
[48] B.I. Schneider, T. N. Rescigno and C.W. McCurdy, Phys. Rev. A **42**, 3132 (1990).

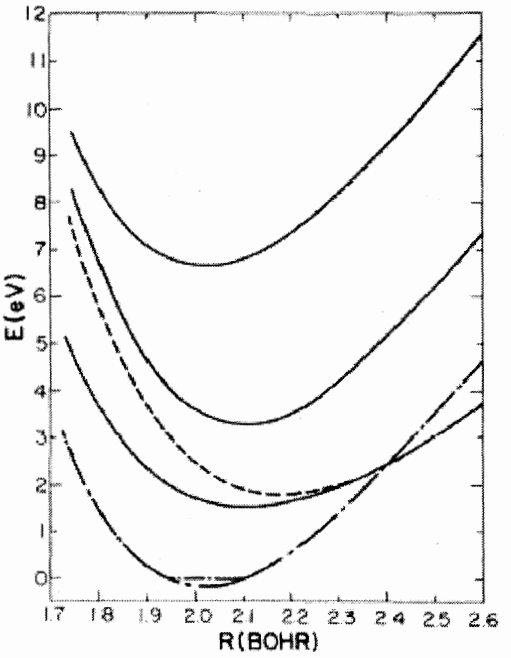

Potential curves for N_2 and N_2^-: Dash-dotted line, ground state of N_2; dotted line, resonant state of N_2^-; and solid line, *R*-matrix states of N_2^-.

Fig. 4: The R-Matrix Potential Curves

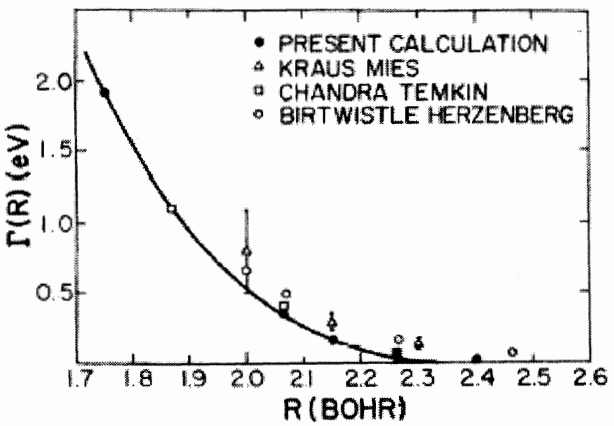

Width resonance as a function of internuclear distance in N_2.

FIG. 5: Resonance Width for e + N_2 Scattering

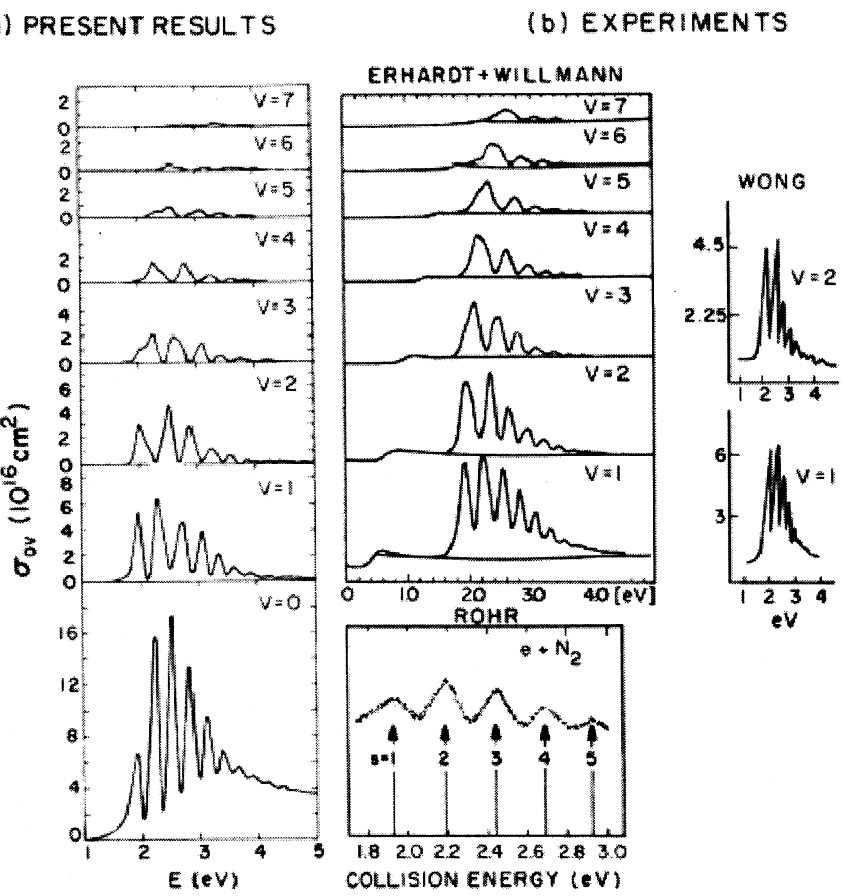

Comparison of calculated and experimental vibrational excitation cross sections for N_2.

FIG. 6: Calculated versus Experimental Vibrational Excitation Cross Section for e + N_2 Scattering

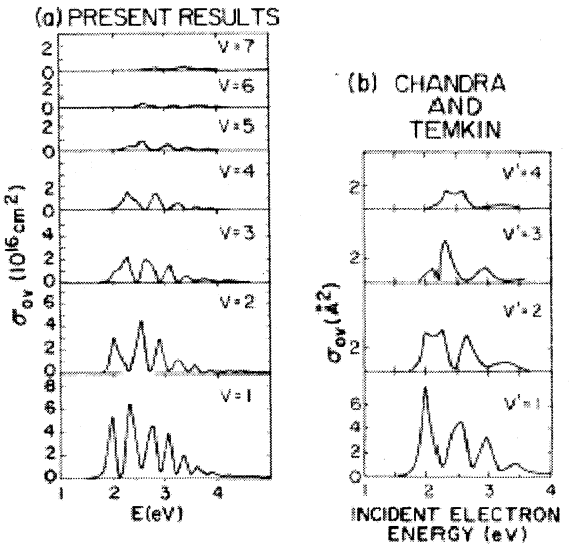

Comparison of calculated cross sections for vibrational excitation in N_2.

FIG. 7: Comparison of R-matrix and Hybrid Theory Vibrational Excitation Cross Section for e + N_2 Scattering

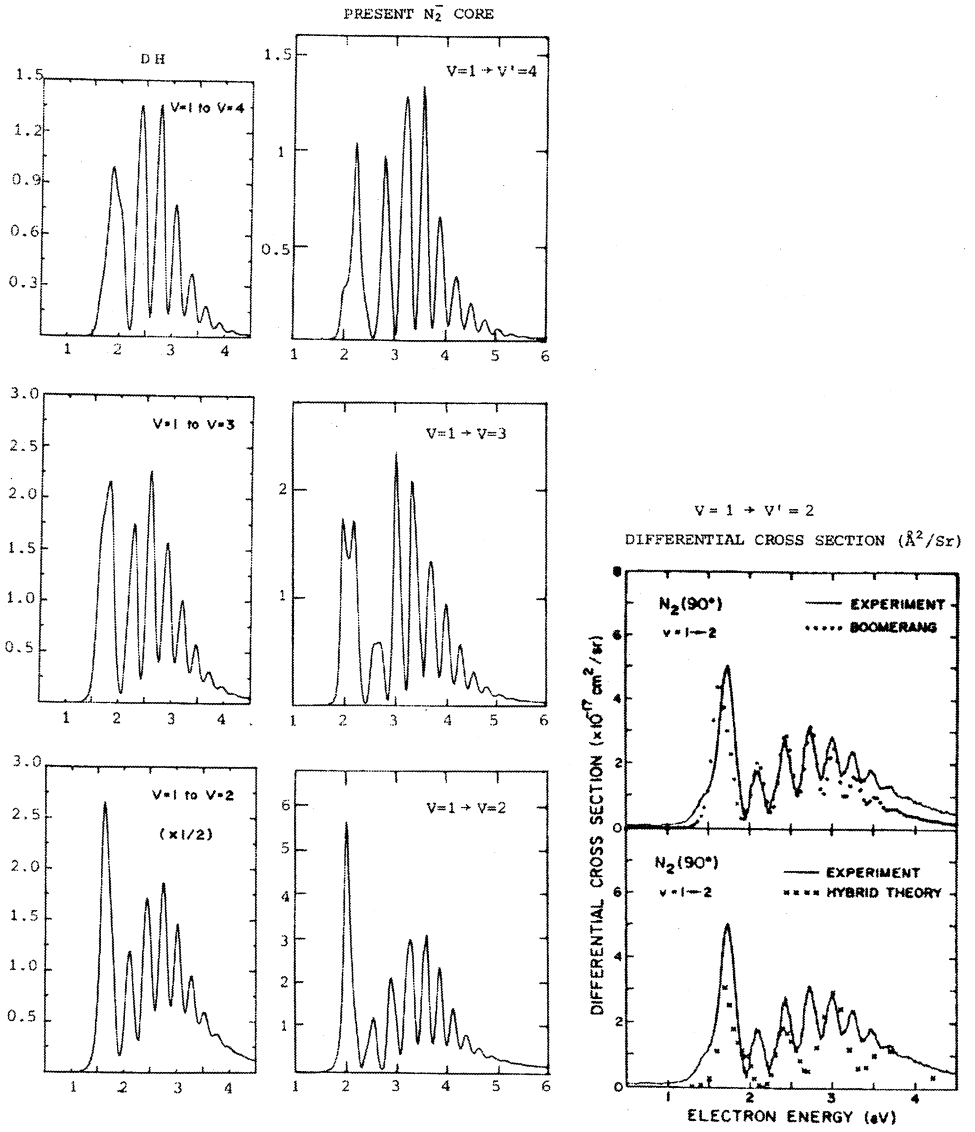

Vibrational excitation cross sections $c_{1\to v}(\text{Å}^2)$
a. Dubé Herzenberg (DH) Boomerang results.
b. N_2^- core approximation present results.
c. Comparison of Wong's experimental results with Dubé–Herzenberg and Chan dra–Temkin theoretical results.

FIG. 8: Calculated and Experimental Excited State Vibrational Excitation Cross Section for e + N_2 Scattering

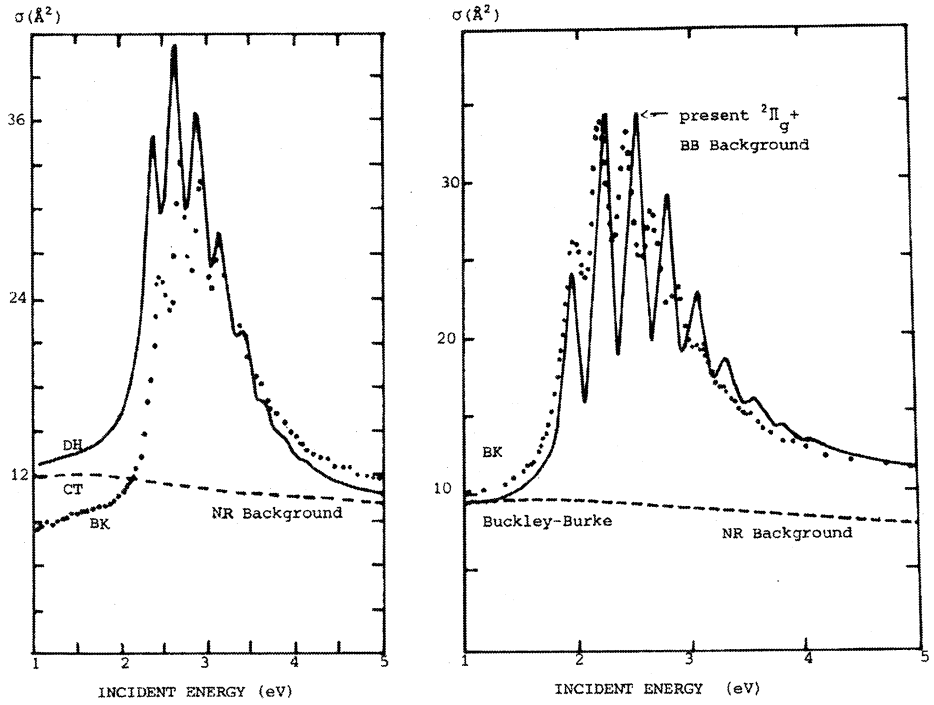

The total scattering cross section ($Å^2$) for e+N_2 (v=0)

a. Bonham and Kennerly (• • •) compared with the theoretical sum (———) of Dubé–Hertzenberg $^2\prod_g$ resonant results and Chandra–Temkin non-resonant background (--------).

b. Bonham and Kennerly experimental results (• • •) compared with the theoretical sum (———) of the present N_2^- core $^2\prod_g$ resonant results and Buckley–Burke non-resonant background (--------).

FIG. 9: The Total Cross Section for e + N_2 Scattering

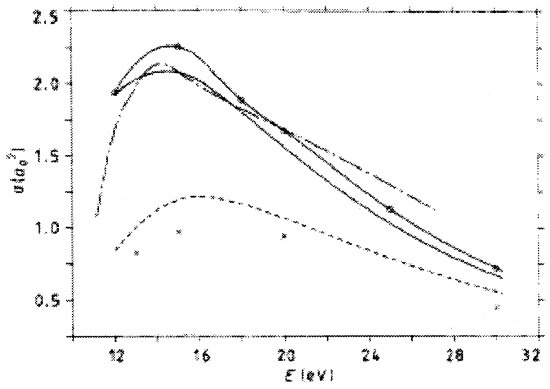

Comparison of theoretical calculations of the X $^1\sum_g$–b $^3\sum_\mu$ total excitation cross sections as a fnction of incident electron energy for e–H_2 scattering. Nomenclature: full curve, present SEC calculations; broken curve, present OSE; chain curve, SEC (Baluja et al. 1985); full curve with circles, SEC (Lima et al. 1985); crosses, OSE (Holley et al. 1981).

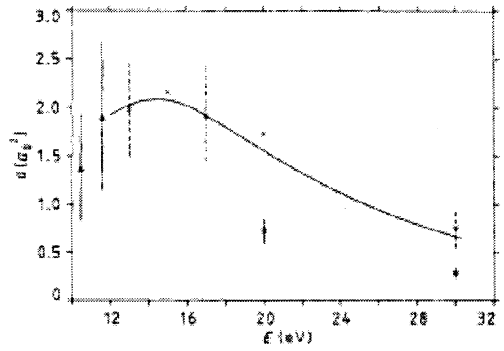

Comparison of theoretical and experimental X $^1\sum_g^+$–b $^3\sum_\mu$ cross sections, Nomenclature: full curve, present SEC calculations; circles, experimental results (Khakoo et al. 1985); crosses, experimental results (Nishimura et al. 1985); triangles, experimental results (Hall and Andrié 1984).

FIG. 10: Electronically Inelastic Scattering from the X $^1\Sigma_g^+$ State to the b $^3\Sigma_u^+$ State of H_2

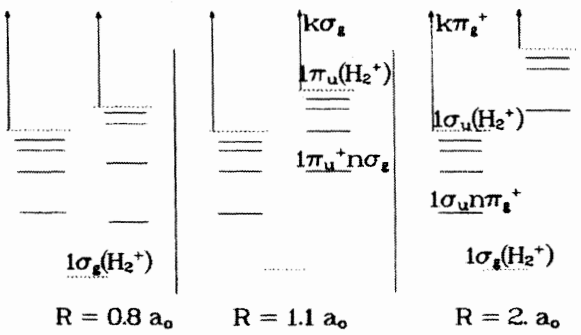

Schematic representation for the $^1\prod_u$ symmetry of the $1\sigma_u n\pi_g^+$ and $1\pi_u^+ n\sigma_g$ Feshbach resonance series of H_2^+ lying below the $1\pi_u$ threshold for $e^- - H_2^+$ scattering as a function of *R*. The resonances are depicted by solid lines, the states of H_2^+ by dashed lines.

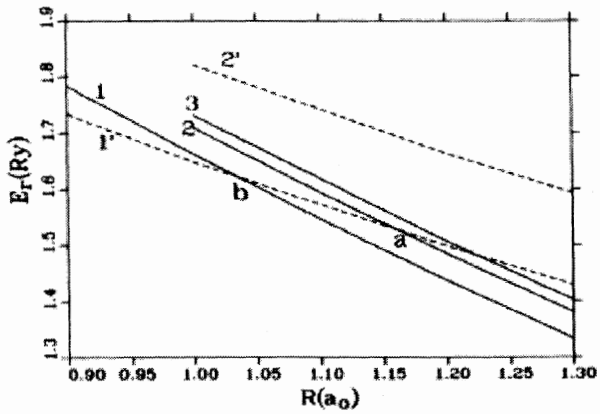

Resonant position E_r as a function of R for the lowest few $^1\prod_u$ resonances in the $1\sigma_u n\pi_g^+$ (solid lines) and $1\pi_u^+ n\sigma_g$ (dashed lines) series in 2CC. The numbers give the order of the resonances within each series.

FIG. 11: Structure of the Double Excited Resonant State of the $^1\Pi_u$ States H_2

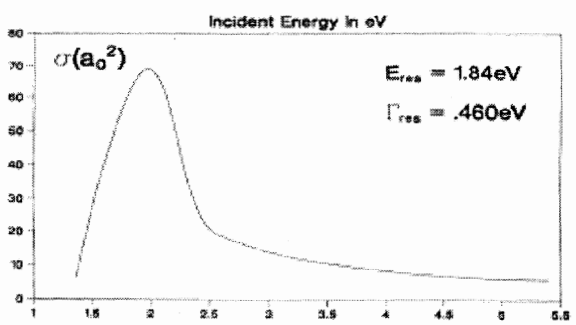

$^2B_{2g}$ partial integrated cross section for $e^- - C_2H_4$ scattering.

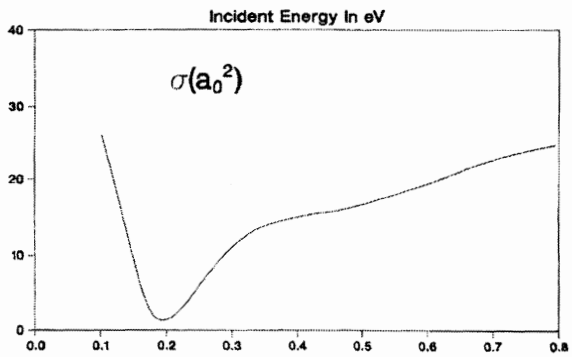

^2A_g partial integrated cross section for $e^- - C_2H_4$ scattering.

FIG. 12: Cross Section for Elastic Electron Scattering from Ethylene

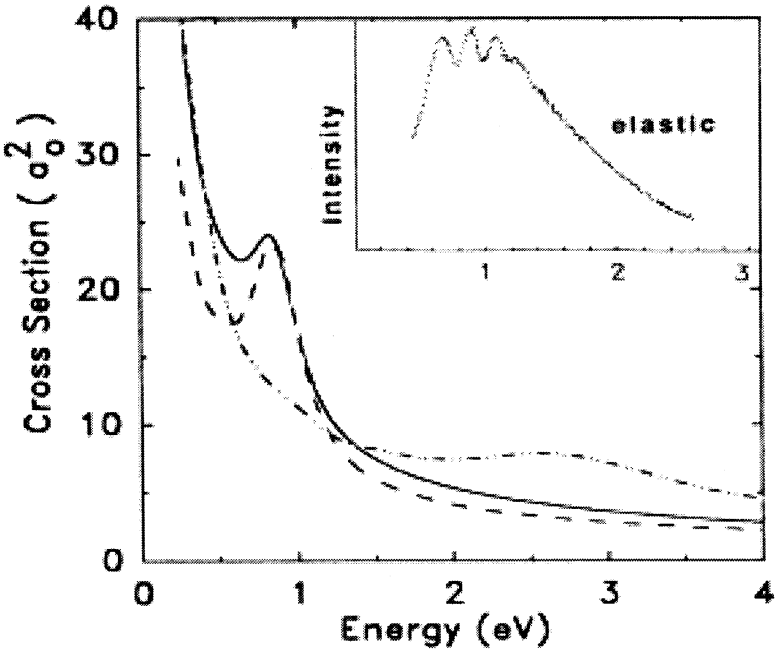

Elastic differential cross section for e^-–CH_2O. Solid Curve: optical-potential results at 90°; dashed curve: optical-potential results at 120°; dash-dotted curve: static-exchange result at 90°. Inset: Experimental results of Benoit and Abouaf (Ref. 8).

FIG. 13: Cross Section for Vibration Excitation in Formaldehyde